ANL–HEP–PR–08–46
EFI–08–22
FERMILAB–PUB–08–269–T

Light Stop Searches at the LHC in Events with One Hard Photon or Jet and Missing Energy

M. Carena[1], A. Freitas[2,3,4] and C.E.M. Wagner[3,4]

[1] *Fermi National Accelerator Laboratory, P.O. Box 500, Batavia, IL 60510, USA*

[2] *Department of Physics, 100 Allen Hall University of Pittsburgh, Pittsburgh, PA 15260, USA*

[3] *HEP Division, Argonne National Laboratory, 9700 Cass Ave., Argonne, IL 60439, USA*

[4] *Enrico Fermi Institute and Kavli Institute for Cosmological Physics, Department of Physics, University of Chicago, 5640 S. Ellis Ave., Chicago, IL 60637, USA*

Abstract

Low energy supersymmetric models provide a solution to the hierarchy problem and also have the necessary ingredients to solve two of the most outstanding issues in cosmology: the origin of the baryon asymmetry and the source of dark matter. In the MSSM, weak scale generation of the baryon asymmetry may be achieved in the presence of light stops, with masses lower than about 130 GeV. Moreover, the proper dark matter density may be obtained in the stop–neutralino co-annihilation region, where the stop–neutralino mass difference is smaller than a few tens of GeV. Searches for scalar top quarks (stops) in pair production processes at the Tevatron and at the Large Hadron Collider (LHC) become very challenging in this region of parameters. At the LHC, however, light stops proceeding from the decay of gluino pairs may be identified, provided the gluino mass is smaller than about 900 GeV. In this article we propose an alternative method for stop searches in the co-annihilation region, based on the search for these particles in events with missing energy plus one hard photon or jet. We show that this method is quite efficient and, when complemented with ongoing Tevatron searches, allows to probe stop masses up to about 160 GeV, fully probing the region of parameters consistent with electroweak baryogenesis in the MSSM.

1 Introduction

Supersymmetric extensions of the Standard Model (SM) provide a natural explanation for dark matter. Stability of the lightest supersymmetric particle (LSP) is ensured by a discrete symmetry, R-Parity. Due to the renormalization group evolution of the supersymmetric particle masses, the LSP is naturally neutral and weakly interacting, and therefore has an annihilation cross section of the order of the one necessary for the LSP to become a good dark matter candidate.

Low energy supersymmetry also provides a possible solution to another outstanding problem of the Standard Model, namely the generation of the baryon-antibaryon asymmetry [1,2]. In the minimal supersymmetric extension of the SM (MSSM), a solution to this problem by weak scale physics demands a light stop as well as non-vanishing CP-violating phases in the chargino–neutralino sector. Such a light stop tends to push the lightest CP-even Higgs mass to values below the current experimental bound [3], unless the heaviest stop mass is larger than about 10 TeV. All other squarks and sleptons should also be heavy, in order to suppress the electron and neutron electric dipole moment contributions [4–6].

The required low energy theory that leads to an explanation of the origin of dark matter and the baryon asymmetry contains the SM particles, a light stop, and light electroweak gauginos and higgsinos, the latter being important for the generation of the CP-violating currents contributing to the baryon asymmetry, as well as a source of dark matter and a light Higgs. Although the scenario does not lead to a prediction for the non-SM Higgs masses, large values of these masses, above a few 100 GeV, provide a natural suppression of the two-loop contribution to the electron electric dipole moments and help in obtaining a sufficiently large value of the lightest CP-even Higgs mass. For large CP-odd Higgs boson masses, the lightest CP-even Higgs will behave in a standard way, and therefore evidence of its presence may appear at the latest phase of the Tevatron collider and should be observed in the next few years at the LHC. However, the effective couplings of the lightest Higgs boson to gluons and photons are modified by a light stop [7], and the measurement of processes involving these couplings could provide evidence for strongly interacting new particles with relatively low mass.

More challenging is the direct search for a scalar top quark. Acceptable values of the relic density for heavy CP-odd Higgs bosons are naturally obtained in the stop–neutralino co-annihilation region, in which the neutralino-stop mass difference is of about a few tens of GeV [5]. In this case, the three-body stop decay channel into W boson, bottom quark and the lightest neutralino is kinematically closed, and the loop-induced two-body decay into a charm and a neutralino tends to be the dominant stop decay mode [8]. Searches for a stop decaying into a charm plus missing energy at the Tevatron collider rely on a sufficiently energetic charm quark, in order to trigger on these events. The charm transverse energy, in turn, is controlled by the mass difference of the stop and the neutralino. For mass differences below 40 GeV, the Tevatron has no sensitivity in stop searches [9]*. For larger mass differences, however, the Tevatron reach extends up to values well above the LEP limit

*Very recently, however, it was proposed that the reach of the Tevatron for small mass differences could be extended by not requiring full reconstruction of the two charm jets [10].

of 100 GeV, allowing to explore stop masses up to 160 GeV [11].

Searches at the LHC in stop pair production are equally challenging. However, at the LHC the stop may be produced in decays of heavy gluinos. Since the gluino is a Majorana particle, it can decay into both a stop–antitop and top–antistop final states. Pair production of gluinos may then lead to a pair of equal-sign top quarks plus two equal-sign stops. It has been shown that these events may be detected for gluino masses below 900 GeV [12, 13].

One would like to explore a method that would not depend so strongly on the assumption of a relatively light gluino, which is not required for either the generation of dark matter or the baryon asymmetry. In this article we propose such a method: Stop particles at the LHC may be produced in association with a hard photon or a hard jet. In the co-annihilation region, there will be minimal hadronic activity associated with the stop decays and therefore this would effectively lead to events with a photon or a jet and missing energy. Such a signature has been proposed, for instance, to explore extensions of the Standard Model by large extra dimensions [14]. Recently, it has been pointed out that the jet plus missing energy signature can also be useful to search for relatively light gluinos at the Tevatron [15]. In this article we show that at the LHC these channels allow to test the whole region of stop and neutralino masses consistent with dark matter and electroweak baryogenesis (EWBG) that cannot be covered by the Tevatron searches.

The article is organized as follows. In section 2 we present an overview of scenarios that accommodate a light stop. The following two sections 3 and 4 are devoted to phenomenological studies of the photon plus missing energy and jet plus missing energy channels at the LHC. In section 5 we shortly comment about the relevance of these channels for the Tevatron. Section 6 compares our results to the reach for stops in gluino decays at the LHC. Section 7 discusses some possibilities for identifying the stops from their decay characteristics at the LHC. Finally, our conclusions are presented in section 8.

2 Scenarios with light scalar top quarks

Although the particle content of minimal supersymmetric extensions of the Standard Model is well defined by symmetry principles, the exact spectrum depends strongly on the scale and nature of the mechanism that leads to the soft supersymmetry breaking parameters. Flavor physics puts strong constraints on the possible structure of supersymmetry breaking terms. Strong flavor changing neutral current effects may be naturally avoided if, at the messenger scale, at which supersymmetry breaking is transmitted to the observable sector, the soft supersymmetry breaking terms are flavor independent. Under these assumptions all squarks and sleptons with the same quantum numbers under the SM gauge group will acquire equal masses at the messenger scale.

The observable supersymmetric particle masses may be obtained by renormalization group evolution of the parameters at the messenger scale to the weak scale. There are different corrections appearing in this evolution [16]. On one hand, strong interaction effects, governed by the gluino mass, drive the squark masses to larger values. There are also Yukawa induced effects that push the third generation squark masses, in particular the stop

masses, to smaller values. These Yukawa effects are the same that drive the effective Higgs mass parameter to negative values, inducing the breakdown of the electroweak symmetry. Once the electroweak symmetry is broken, there is also a Higgs induced mixing between the right-handed and left-handed stops, that pushes the lightest stop to small values. In general, in the scenarios with flavor independent scalar masses at the messenger scale, the lightest stop is the lightest squark, and the precise value of its mass depends on the scale of supersymmetry breaking, the gluino mass and the size of the stop mixing parameter. For relatively small values of the gluino mass and a large stop mixing mass parameter, the lightest stop can have masses of the order or smaller than the top quark mass [17]. Due to the renormalization group evolution such a light stop is dominantly the partner of the right-handed top quark, which also concurs with electroweak precision constraints.

Light stops may also appear in alternative solutions to the flavor problem; Since the strongest flavor physics constraints are associated with the first two generations, a simple solution is to let the first and second generation squark masses to be very large, while the stops remain light, in order to prevent large radiative corrections to the Higgs mass parameter. In these "more minimal supersymmetry" scenarios [18], one considers that these conditions are fulfilled at the weak scale, independently of the gluino mass or the scale of supersymmetry breaking. Observe, however, that unless there are additional interactions beyond the MSSM, one of the stops needs to be heavier in order to prevent a Higgs mass below the experimental bound [3].

One can also consider a phenomenological scenario similar to split supersymmetry [19], in which all superparticles which remain light are there for a reason [20]. In this case, a light stop would be necessary to induce a strongly first-order phase transition, necessary for electroweak baryogenesis, while light Higgsinos and gauginos would be necessary to lead to a dark matter candidate, generate the necessary CP-violating currents and for the model to be consistent with the unification of gauge couplings at high scales.

In all of the above scenarios, additional assumptions have to be made about the sfermion flavor structure to predict the width and branching ratios of the light stop. For this work, it is assumed that the two-body decay $\tilde{t}_1 \to c + \tilde{\chi}_1^0$ is enhanced by large logarithms from renormalization group evolution [8, 21] so that this decay channel becomes dominant and the stop decay length is too short to be observable. Alternative scenarios where the partial width for $\tilde{t}_1 \to c\,\tilde{\chi}_1^0$ is small lead to interesting signals from the competing four-body decay $\tilde{t}_1 \to b\,l^+\nu_l\,\tilde{\chi}_1^0$ and displaced stop decays [21] but will not be investigated further here.

3 Stops in the $\gamma + \not{E}_{\mathrm{T}}$ channel

As explained in the previous section, we are interested in exploring stop production in the co-annihilation region, where the mass difference between the stop and the lightest supersymmetric particle, which we assume to be the neutralino $\tilde{\chi}_1^0$,

$$\Delta m = m_{\tilde{t_1}} - m_{\tilde{\chi}_1^0}, \tag{1}$$

is of the order of a few tens of GeV. In this region, the visible decay products of the stop tend to be soft, and therefore difficult to observe at hadron colliders. However, the lack of

hadronic activity in the stop decay products may be useful in searches for stops in other channels, for instance by looking at the recoil of stops against a hard photon or jet. In this section, we shall explore the possible production of a stop in association with a hard photon. Since the stop decays into relatively soft jets and missing energy, the final state in the stop production channel may be taken as $\gamma + \not{E}_{\rm T}$. We have therefore performed the simulation of the signal

$$p\,p \to \tilde{t}_1\,\tilde{t}_1^*\,\gamma \tag{2}$$

using CompHEP 4.4 [22], interfaced with Pythia 6.4 [23] through the CPyth toolkit 2.0.6 [24]. Pythia has been run with power showers and including stop fragmentation and hadronization [25] before decay $\tilde{t}_1 \to c + \tilde{\chi}_1^0$. The Pythia output has been fed into the fast detector simulation PGS [26], in order to simulate the most important detector effects.

The $\gamma + \not{E}_{\rm T}$ signature has been considered previously for searches for large extra dimensions at the LHC [27,28]. Therefore we can use the published results for the evaluation of the Standard Model background at the LHC. Our analysis is based on the SM background estimates by the CMS collaboration in Ref. [27]. The main physics background channels come from the production of weak gauge bosons, for instance, γZ with $Z \to \nu\bar{\nu}$, and $W \to e\nu$ where the electron is faking a photon. These channels may be calibrated from observations in other well measured production processes. For instance, γZ with $Z \to \nu\bar{\nu}$ can be calibrated from γZ with $Z \to l^+l^-$ with a total error of 3% [27], using extrapolation from small $p_{{\rm T},\gamma}$ to the signal region.

Since all colored particles, including gluinos and other squarks, are considered to be heavy, with masses of about 1 TeV or larger, the potentially large SUSY contributions to the background associated with color particle production are assumed to be negligible after applying the analysis cuts. The main irreducible SUSY background stems from the production of neutralinos with photons, which is, again, numerically small and can be neglected compared to the SM backgrounds.

In order to obtain a reliable estimate of the expected stop signal significance at the LHC, our analysis has been performed using similar cuts as the ones used in the CMS study, Ref. [27]:

1. Require one hard photon with $p_{\rm T} > 400$ GeV and pseudo-rapidity $|\eta| < 2.4$.
2. Missing energy requirement: $\not{E}_{\rm T} > 400$ GeV.
3. Veto against tracks with $p_{\rm T} > 40$ GeV.
4. Require back-to-back topology for photon and missing momentum: $\Delta\phi(\not{\vec{p}}_{\rm T}, \vec{p}_\gamma) > 2.5$.
5. The photon has to be isolated. Ref. [27] uses a likelihood method for photon isolation, but for simplicity we use the standard isolation criteria in PGS [26]. The impact of these details on the signal is small.

After applying these cuts, the remaining SM background is relatively small, about 2.5 fb, corresponding to 250 events for 100 fb^{-1} [27].

$m_{\tilde{t}_1}$/GeV =	110	130	150	170	190	210	230
Δm/GeV = 10	189	173	157	138	114	103	85
20	111	119	110	99	86	81	71
30	72	74	77	80	64	60	57
40	56	54	55	53	48	45	45
50	43	43	40	40	37	35	34

Table 1: *Number of signal events in the $\gamma + \not{E}_{\rm T}$ channel for 100 fb^{-1} and for various combinations of $m_{\tilde{t}_1}$ and $\Delta m = m_{\tilde{t}_1} - m_{\tilde{\chi}_1^0}$. The numbers in the table have an intrinsic statistical uncertainty of a few events from the Monte Carlo error.*

The above cuts, however, also affect the signal rate, particularly for increasing values of Δm due to the strong $\not{E}_{\rm T}$ requirement established above. One could in principle optimize the cuts as a function of Δm, but this would require a reevaluation of background, which is beyond the scope of this paper. Since no cut optimization has been performed, the procedure we are applying serves therefore as a conservative estimate of the reach in the stop–neutralino mass parameter space.

Although the SM backgrounds are known including next-to-leading (NLO) QCD corrections, no such corrections are available for the $\tilde{t}_1\tilde{t}_1^*\gamma$ process. In our analysis, we shall assume a K-factor of 1.4, an estimate that comes from the calculation of the process $pp \to \tilde{t}_1\tilde{t}_1^*$ [29]. However, this value should be taken with caution since the veto of any hard real radiation jets due to our selection cuts could reduce the effective size of the radiative corrections, an effect that is partially but not precisely reproduced by the parton shower in PYTHIA[†].

After application of the cuts and the K-factor rescaling the signal event number for 100 fb^{-1} is shown in Tab. 1 for various values of the stop and neutralino masses. Figure 1 shows the distribution of the photon transverse energy for the SM background and the stop signal for $m_{\tilde{t}_1} = 130$ GeV and $m_{\tilde{\chi}_1^0} = 110$ GeV (*i.e.* $\Delta m = 20$ GeV). As can be seen from the figure, the shape of the $E_{{\rm T},\gamma}$ distribution is very similar for the background and stop signal, so that the only discriminating feature is the overall event count.

Using this information, the projected reach for stop searches by means of the procedure explained above is represented in Fig. 2 without (left) and with (right) systematic errors. In Fig. 2 we have considered the following systematic errors:

- Assuming a 2% error on the measaurement of the photon $p_{\rm T}$ leads to a 3% uncertainty of the SM background. The estimate has been obtained by simulating events for the dominant background γZ with $Z \to \nu\bar{\nu}$ and it agrees well with the evaluation in Ref. [27].

- Assuming a 5% error on the measurement of $\not{E}_{\rm T}$, we obtain an effect of 5% on the

[†]Due to the missing NLO corrections, our evaluation of the $\gamma + \not{E}_{\rm T}$ channel has sizable theoretical uncertainties. However, the jet+$\not{E}_{\rm T}$ channel, discussed in the next section, gives much better and more robust results.

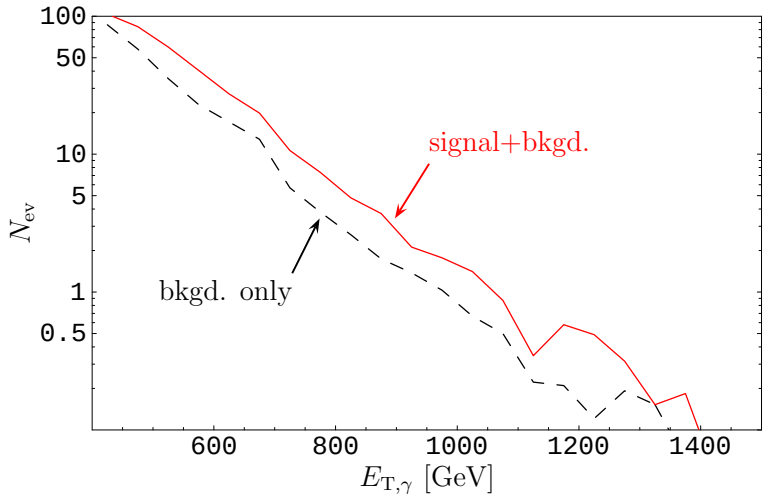

Figure 1: *Distribution of the photon transverse energy, $E_{\rm T,\gamma}$, for the SM background (from Ref. [27]) and the stop signal with $m_{\tilde{t}_1}$=130 GeV and $m_{\tilde{\chi}_1^0}$=110 GeV. The fluctuations at the right end of the plot are due to Monte Carlo errors.*

background, which is slightly larger than the number of 4% quoted in Ref. [27].

- A precise determination of parton distribution functions (PDFs) is crucial for the measurement of the $\gamma+\not{E}_{\rm T}$ cross section. We expect that the PDFs can be constrained by measurements of the reference process γZ with $Z \to l^+l^-$. Therefore the systematic error due to PDFs should be similar to the statistical error of that process, *i.e.* about 3%.

Adding the individual contributions in quadrature, the total systematic error is expected to be about 6.5%.

Figure 2 shows the 5σ discovery reach with the statistical significance estimated by $S/\sqrt{B}$. Also shown are current [9] and projected [11] 95% confidence level (C. L.) exclusion limits for light stop searches in the jets plus missing energy channel at the Tevatron collider. Observe that since Tevatron searches are more efficient for large values of Δm, while the LHC searches explored in this article become more efficient for small values of Δm, searches for stops at both colliders complement each other. High luminosities at both hadron colliders allow to probe a large fraction of the region of stop–neutralino masses consistent with electroweak baryogenesis, $m_{\tilde{t}_1} < 130$ GeV. This is particularly so in the co-annihilation region, but can be applied to larger values of Δm if the systematic errors discussed above were reduced, getting results close to the left panel of Fig. 2.

4 Stops in the jet+$\not{E}_{\rm T}$ channel

The search for photons and $\not{E}_{\rm T}$ explored in the last section could be a promising way of looking for stops in the co-annihilation region. However, the reach is limited due to the

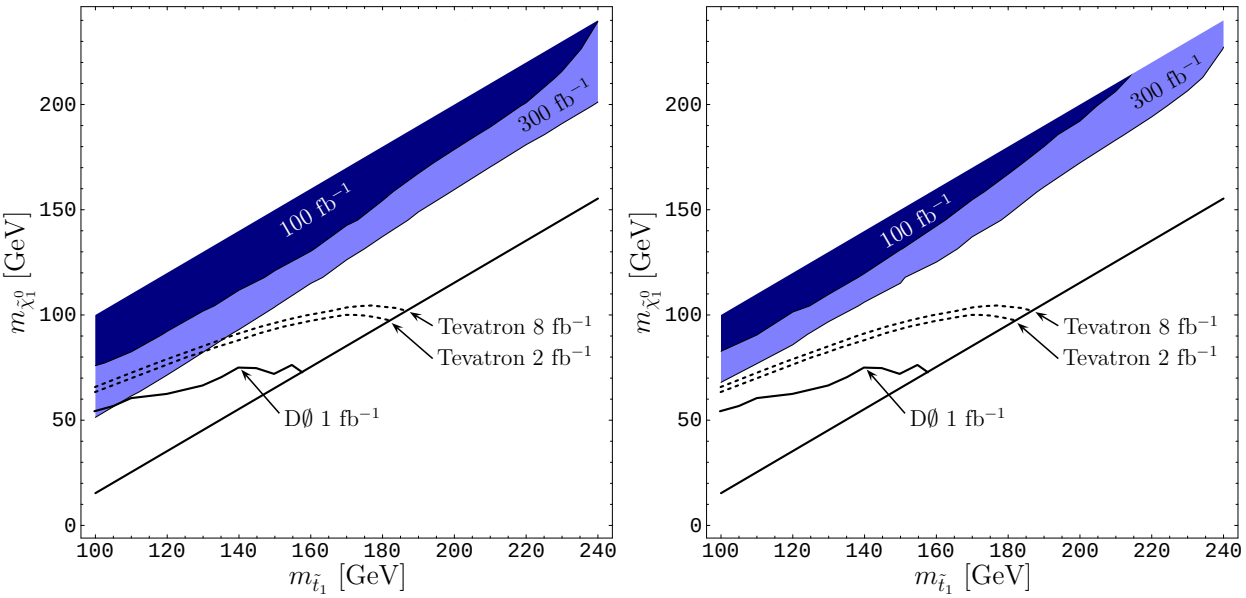

Figure 2: *Projected LHC 5σ discovery reach in the $\gamma + \not{E}_{\rm T}$ channel without (left) and with (right) systematic errors. For comparison the current and future Tevatron 95% C. L. exclusion bounds for light stops are also shown.*

relatively small signal cross section. An alternative method, with similar properties as the searches discussed above is to look for the recoil of stops against hard jets. An advantage of this search channel compared to the $\gamma + \not{E}_{\rm T}$ is the much larger rate induced by the strong interaction production process. A clear disadvantage, however, is related to larger measurement uncertainties, and increased backgrounds and systematic errors. In particular, to control the potentially large QCD background, large missing transverse energy $\not{E}_{\rm T} > 1$ TeV must be demanded.

Due to the small hadronic activity associated with the decaying stop, and analogously to the photon case, the main signature of this process is

$$pp \to \text{jet} + \not{E}_{\rm T}. \tag{3}$$

As in the photon case, we have performed a Monte Carlo simulation of this discovery channel. The signal $\tilde{t}_1\tilde{t}_1^* + j$ has been generated using CompHEP 4.4 [22], interfaced with Pythia 6.4 [23]. No matching procedure has been applied for jet radiation from matrix elements and parton showers, but errors due to that should be small since the typical $p_{\rm T}$ for the hardest jet is very large to balance the large $\not{E}_{\rm T}$.

As in the photon case, we have extracted the SM backgrounds from previous experimental studies at the LHC. The jet+$\not{E}_{\rm T}$ channel has been investigated in searching for large extra dimensions in Ref. [28], which also contains a detailed analysis of SM backgrounds. The main physics background channels are also similar to the photon case : jZ with $Z \to \nu\bar{\nu}$, and jW with $W \to \tau\nu$. Here j stands for a hard jet. The process jZ with $Z \to \nu\bar{\nu}$ can be

$m_{\tilde{t}_1}$/GeV =	110	130	150	170	190	210	230
Δm/GeV = 10	1920	1716	1585	1360	1056	1015	845
20	1170	1085	948	877	717	676	570
30	762	746	676	679	548	551	433
40	559	516	514	507	442	444	348
50	437	449	422	428	364	343	279

Table 2: *Number of signal events in the jet+$\not{E}_{\rm T}$ channel for 100 fb^{-1} and for various combinations of $m_{\tilde{t}_1}$ and $\Delta m = m_{\tilde{t}_1} - m_{\tilde{\chi}_1^0}$. The event numbers in the table have an intrinsic statistical uncertainty of a few tens from the Monte Carlo error.*

calibrated from jZ with $Z \to l^+l^-$ [28], and for similar reasons as in the photon case, the SUSY background has been assumed to be small.

In order to proceed with this analysis, we have used the same cuts as in Ref. [28]:

1. Require one hard jet with $p_{\rm T} > 100$ GeV and $|\eta| < 3.2$ for the trigger.
2. Large missing energy $\not{E}_{\rm T} > 1000$ GeV.
3. Veto against electrons with $p_{\rm T} > 5$ GeV and muons with $p_{\rm T} > 6$ GeV in the visible region ($|\eta| < 2.5$).
4. Require the second-hardest jet to go in the opposite hemisphere as the missing momentum (*i.e.* the first and second jet should go in roughly the same direction): $\Delta\phi(p_{\rm T,j_2}, \vec{p}_\gamma) > 0.5$. This cut reduces background from $W \to \tau\nu$ where the tau decay products are emitted mostly in the opposite direction as the hard initial-state jet.

Application of these cuts leads to a SM Background of about 7 fb, corresponding to 700 events for 100 fb^{-1} [28].

The NLO corrections to $\tilde{t}_1\tilde{t}_1^* + j$ are not available in the literature. However, experience from $t\bar{t}j$ [30] suggests that the K-factor should be close to one. Therefore, contrary to what was done in the photon case, we shall not include a K-factor for the signal.

Using the above defined cuts, the expected number of signal events is listed in Tab. 2 for various stop and neutralino mass values. Fig. 3 shows the projected 5σ discovery reach with the statistical significance estimated by $S/\sqrt{B}$ and including systematic errors. In order to estimate the systematic errors, we have explored the following two strategies, (a) and (b):

(a) The first strategy determines the dominant SM backgrounds directly from data [28]. In particular, the jZ background with $Z \to \nu\bar{\nu}$, which contributes about 75% of the SM background after cuts, can be inferred from jZ with $Z \to l^+l^-$, $l = e, \mu$. The $Z \to l^+l^-$ calibration channel is about seven times smaller than the $Z \to \nu\bar{\nu}$ background in the signal region ($p_{{\rm T},ll} > 1$ TeV), thus leading to the error estimate $\delta_{\rm sys}B = \sqrt{7B}$.

(b) Alternatively, similar to the previous section, individual systematic error sources can be identified:

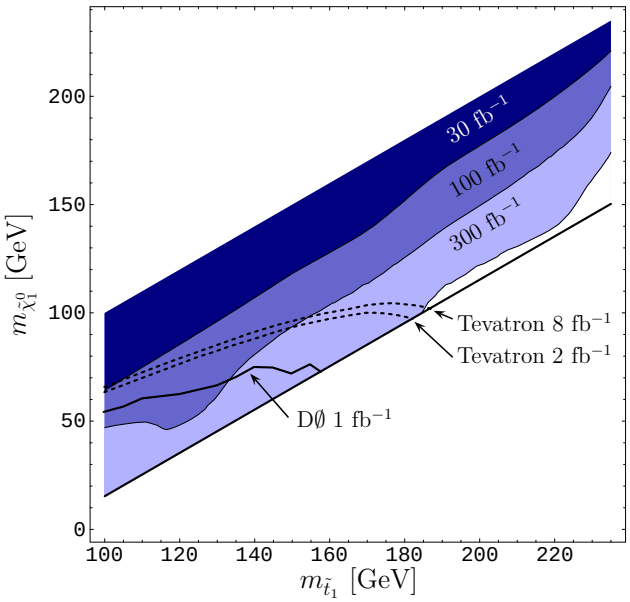

Figure 3: *Projected LHC 5σ discovery reach in the jet+$\not{E}_{\rm T}$ channel. For comparison the current and future Tevatron 95% C. L. exclusion bounds for light stops are also shown.*

- A 5% error on $\not{E}_{\rm T}$ induces a 36% uncertainty on the background, as determined by simulating jZ with $Z \to \nu\bar{\nu}$.
- The PDFs can be extracted from reference SM processes, *e.g.* jZ with $Z \to l^+l^-$. Thus the uncertainty is mainly limited by the statistical error for the standard candle process. For the region of high transverse momenta ($p_{\rm T} > 500$ GeV), which is relevant for the present analysis, this leads to relatively small error of 3%.
- Systematic uncertainties associated with the lepton veto are negligible, since this cut plays a role mainly for the jW background with $W \to e\nu$ or $W \to \mu\nu$, which contributes only about 5% to the total SM background.

In summary, this strategy yields a total estimated systematic error of about 36%, strongly dominated by the uncertainty of the missing $\not{E}_{\rm T}$ measurement.

It is evident that the data-driven method (a) for determining the systematic error of the SM backgrounds leads to better results. This is different from the photon case in section 3, in which method (b) proves to be convenient. The improvement in the results associated with method (a) in the jet case is due to the larger statistics, while on the other hand a much larger background uncertainty is induced for method (b) by the error in the missing energy determination.

The results presented in Fig. 3 make use of method (a). Searches in the jet plus $\not{E}_{\rm T}$ channel turn out to be more promising than in the photon plus $\not{E}_{\rm T}$ channel. They allow to test the co-annihilation region up to relatively large values of the stop mass, of about 200 GeV or larger. Moreover, when complemented with Tevatron search analyses, they

allow to fully explore the region of stop masses consistent with electroweak baryogenesis with only 100 fb^{-1} of integrated luminosity.

5 Stops in $\gamma + \not{E}_{\rm T}$ and jet$+\not{E}_{\rm T}$ at the Tevatron

In principle, the $\gamma + \not{E}_{\rm T}$ and jet$+\not{E}_{\rm T}$ channels could be used already at the Tevatron for searching for stops with small stop-neutralino mass difference, a region of parameter space which is difficult to access with traditional search strategies.

Using CompHEP 4.4 [22], we have computed the stop signal cross section for the Tevatron in these channels, and have compared them to the background evaluations by the CDF [31] and D$\emptyset$ [32] collaborations.

For the $\tilde{t}_1\tilde{t}_1^* + \gamma$ channel with a stop mass of $m_{\tilde{t}_1} = 100$ GeV, the Tevatron cross section for $p_{{\rm T},\gamma} > 90$ GeV and $|\eta_\gamma| < 1$ is about 3.2 fb, which is of the same order as the systematic error in the background analysis of CDF ($\delta_{\rm sys} = 1.5$ fb) and D$\emptyset$ ($\delta_{\rm sys} = 1.5$ fb). For larger values of $m_{\tilde{t}_1}$ the signal cross section is even smaller.

In the $\tilde{t}_1\tilde{t}_1^* + j$ channel with $m_{\tilde{t}_1} = 100$ GeV and the minimal cut $p_{{\rm T},{\rm j}_1} > 150$ GeV the Tevatron cross section is about 50 fb, which is smaller than the estimated systematic error on the SM background of 56 fb [31].

Our conclusion is that the Tevatron will not be able to discover stops via the $\gamma + \not{E}_{\rm T}$ or jet$+\not{E}_{\rm T}$ channels. However, searches in the $\gamma + \not{E}_{\rm T}$ signature could exclude light stops with $m_{\tilde{t}_1} \sim 100$ GeV at the 95% confidence level. A final statement about exclusion limits would require a more detailed experimental analysis.

6 Stops in gluino decays

As has been proposed in Refs. [12, 13], if gluinos are light enough, stops can be discovered in their decays. Due to the Majorana nature of gluinos, they may decay in two CP-related channels,

$$\tilde{g} \to \tilde{t}_1\bar{t},\ \tilde{t}_1^* t. \tag{4}$$

One can therefore make use of this property to look for same-sign top quark signatures (using leptonic W decays) plus missing energy in gluino pair production processes. Same-sign top quark channels have much smaller backgrounds than the opposite-sign top quark processes, and allow an efficient search for light stops for relatively light gluinos.

For the sake of comparison to our results in the previous sections, in this section, we re-evaluate the LHC stop discovery reach in this process, using the same cuts as in Ref. [12]:

- Two same-sign leptons with $p_{\rm T} > 20$ GeV.
- At least *(a)* two or *(b)* four jets with $p_{\rm T} > 50$ GeV. The two-jet selection (a) preserves more of the signal for small Δm, while the four-jet selection (b) gives a better signal-to-background ratio for $\Delta m \gtrsim 10$ GeV. For a given MSSM scenario, we always choose the selection method (a) or (b) which gives a better signal significance.

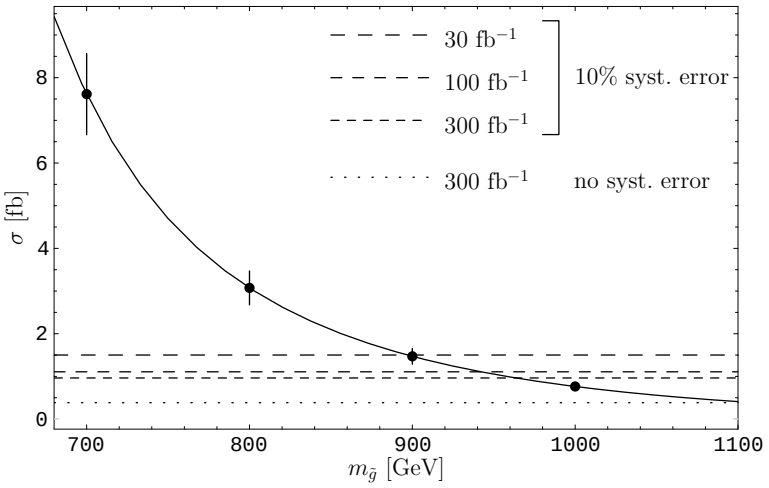

Figure 4: *Projected LHC reach in the $\tilde{g}\tilde{g} \to tt\tilde{t}_1^*\tilde{t}_1^*$ ($\overline{tt}\tilde{t}_1\tilde{t}_1$) channel. The errors bars indicate Monte Carlo errors.*

- At least 2 b-tagged jets with $p_{\rm T} > 50$ GeV. It has been assumed that the b-tagging efficiency is 43% per bottom jet, while the mis-tagging rates are 10% for charm jets and 2.5% for light-flavor jets.
- $\not{E}_{\rm T} > 100$ GeV.
- Two combinations of lepton and b-jet momenta have to give $m_{bl} < 160$ GeV, in order to reduce non-top background.

Using PYTHIA 6.4 [23] interfaced with PGS [26], we were able to reproduce the signal numbers in Ref. [12] within Monte Carlo errors.

Scanning over a wide range of sparticle masses, we found that the expected discovery reach of the LHC in this channel depends only mildly on stop and neutralino masses, but strongly on the gluino mass. In Figure 4, we present the results of our analysis. These results suggest that, as already stated in Ref. [12], for 30 fb^{-1}, the stop reach in this channel extends to about $m_{\tilde{g}} = 900$ GeV. Higher luminosities at the LHC allow to slightly extend the region of gluino masses, but, after considering systematic errors, still gluino masses $m_{\tilde{g}} < 1$ TeV would be required for an efficient search for stops in this channel. Here we have assumed a systematic error of 10% on the remaning SM background after cuts, which is dominated by $t\bar{t}$. The major systematic uncertainty for this background stems from the measurement of $\not{E}_{\rm T}$; a 5% error on $\not{E}_{\rm T}$ induces an uncertainty of 10% on the $t\bar{t}$ rate.

7 Stop identification at the LHC

In the previous sections we have analyzed the possible searches for stops in associated production with hard photons or jets at the LHC. If an excess in these channels were observed, it would be very important to be able to determine that indeed stops, and not other particles,

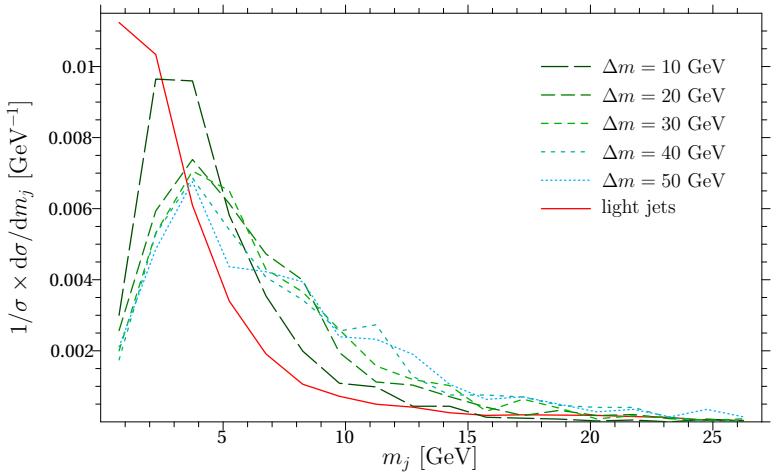

Figure 5: *Jet mass distribution for charm jets from stop decays for different Δm, compared to light flavor jets from ISR.*

are the source of the missing energy events. In order to do this, one would have to detect the relatively soft charm jets coming from the stop decay $\tilde{t}_1 \to c\,\tilde{\chi}_1^0$.[‡]

In the following we shall attempt to identify the charm-jets by means of jet mass and track multiplicity. We focus on the $\gamma + \not{E}_{\mathrm{T}}$ study as an example, and look at the soft jets that survive the track veto and other selection cuts. For each jet its mass is calculated as the invariant mass of the momentum vectors associated with the calorimeter hits inside the jet cluster.

Fig. 5 shows the jet mass distribution for charm jets from stop decays for different values of Δm, and for light-flavor jets from initial state radiation (these light ISR jets come both from signal and background). As evident from the figure, the jet mass distribution is clearly different for light-flavor jets and charm jets. Cutting $m_j > 4.5$ GeV keeps about 60% of the charm jets (for $\Delta m \gtrsim 20$ GeV) but only 25% of light flavor jets.

The distinction between light-flavor and charm jets from the jet mass becomes difficult for very small mass differences $\Delta m \sim 10$ GeV. However, the charm tagging performance can be improved by including other variables in addition to the jet mass. The implementation of a state-of-the-art charm tagging algorithm is beyond the scope of this work, but we have designed a simple two-variable tagging method using the jet mass and track multiplicity within the jet. Track multiplicity as a discriminatory variable is particularly useful for small Δm since in this case the charm jet contains fewer charged tracks than a typical light-flavor jet. This can be explained by the limited phase space available for QCD radiation from a soft charm quark. The results for the tagging efficiency are shown in Tab. 3.

As mentioned above, charm tagging can be used to identify the flavor of the stop decay products. As an example, we have chosen the following sample parameter point: $m_{\tilde{t}_1} = 130$ GeV, $\Delta m = 20$ GeV. The signal can be detected with $> 5\sigma$ with 100 fb^{-1} for this point,

[‡]At an e^+e^- collider, a detailed analysis of stop decays and other properties is possible with high precision [33], but here we want to focus on measurements at the LHC alone.

	Charm jets					Light-flavor jets
Δm [GeV]	10	20	30	40	50	
Efficiency	50%	60%	63%	65%	66%	25%

Table 3: *Charm tagging efficiency and light-jet mistagging rate for a simple tagging algorithm based on jet mass and track multiplicity.*

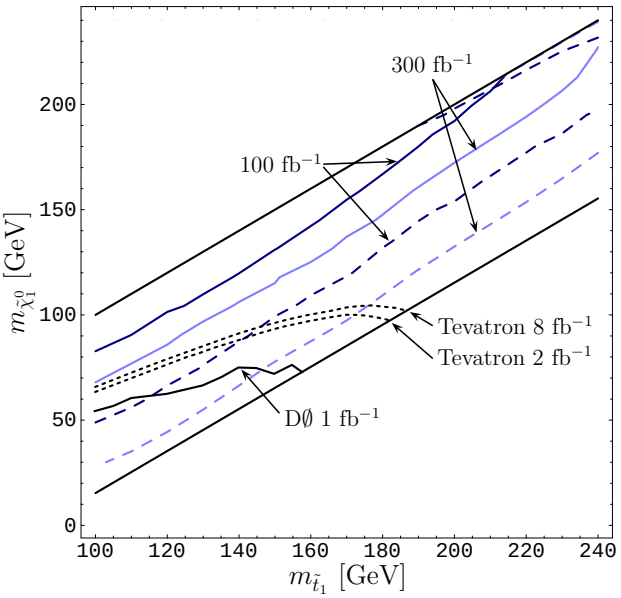

Figure 6: *Improvement of projected LHC reach in the $\gamma + \not{E}_{\rm T}$ channel from charm tagging, for 100 fb^{-1} (dark lines) and 300 fb^{-1} (light lines). The solid lines correspond to the right side of Fig. 2 which has no charm tagging, while the dashed lines indicate the extended reach due to charm tagging as described in the text.*

yielding 119 signal and 251 background events. If only light-flavor jets were present in the entire sample, the requirement of at least one charm-tagged jet with $p_{\rm T} > 20$ GeV would reduce the event count to 23%. In reality, due to the charm jets coming from stop decays, 31.5% survive. This means that the presence of heavy flavor jets in the signal can be inferred experimentally with 2.9σ. With 300 fb^{-1}, this improves to 5σ.

Apart from allowing to determine the flavor of the stop decay product, charm tagging can also improve the stop discovery reach compared to the analysis in section 3, where the decay products of the stops did not play any role in the signal selection. Here, in addition to the cuts in section 3, we demand at least one charm-tagged jet with $p_{\rm T} > 20$ GeV, using the tagging efficiencies in Tab. 3. With this additional cut, we find that the region bounded by the dashed lines in Fig. 6 becomes accessible in the $\gamma + \not{E}_{\rm T}$ channel. As evident from the figure, the discovery region is greatly extended compared to the results from section 3.

Nevertheless, the treatment of charm tagging in this work is rather simple and rudimentary, since we are not using a full detector simulation. A detailed detector simulation is

necessary to evaluate information about displaced vertices, impact parameters and tagged mesons. With a combination of all these variables more sophisticated charm tagging algorithms can be designed which could yield even better results than our analysis.

Once the charm jets are identified one could in principle use kinematical measurements to obtain information about the stop and neutralino masses, see for example Ref. [34]. However, for the $\gamma + \not{E}_{\rm T}$ and jet$+\not{E}_{\rm T}$ channels such an analysis is very difficult due to the relatively small signal-to-background ratio and distortions stemming from the rejection of extra jets in the selection cuts. A conclusive statement about the measurability of the masses would require a detailed study with proper simulation of the backgrounds, which is beyond the scope of this paper.

8 Conclusions

In this article, we have investigated the possible search for light stops in their production in association with hard photons or jets. Light stops may naturally appear in many SUSY scenarios and are required to realize the mechanism of electroweak baryogenesis in the MSSM. These search channels are particularly useful in the case of small mass differences Δm between the stop and the neutralino, for which the jets coming from the decay of the stops are relatively soft. Such small mass differences enable the stop-neutralino co-annihilation process, yielding a dark matter density consistent with experimental observations.

Searches for pair of stops in two jets plus $\not{E}_{\rm T}$ channels at the Tevatron and the LHC require sufficiently hard jets in order to trigger on these events. For small mass differences between the stop and the neutralino these searches become therefore very challenging. The lack of hadronic activity in the stop decay products may be used as an advantage in processes in which the stops are produced in association with photons or jets, since effectively they can lead to final states with one hard photon or jet and missing energy. In this article, we have analyzed such processes. We showed that the photon plus $\not{E}_{\rm T}$ channel may be used to explore most of the light stop co-annihilation region, but it becomes rapidly inefficient for relatively large mass differences Δm, particularly due to the existence of large systematic errors. Searches in the jet plus $\not{E}_{\rm T}$ channel, instead, profit from larger production rates and lead to an extended coverage of the light stop–neutralino mass plane. These searches may be complemented with the Tevatron searches, which become more efficient for larger values of Δm. Together, for an LHC luminosity of about 100 fb^{-1}, they cover all of the parameter space consistent with electroweak baryogenesis, independent of the value of the gluino mass. Since we have used existing experimental simulations for the background evaluation the selection cuts are not optimized for our signal process. An optimization of the cuts thus could further improve our results.

We have also reanalyzed the possibility of looking for stops in events with a pair of like-sign top quarks proceeding from Majorana gluino decays, and have confirmed the results of previous analyses which showed that for an LHC luminosity of 30 fb^{-1}, these searches become efficient for gluino masses below about 900 GeV. Relatively light gluinos, with masses below about 1 TeV, are required even for an LHC luminosity of about 300 fb^{-1}.

In the searches described above the stop properties are not well identified in these processes. Therefore, we have also analyzed the possibility of identifying stops, once an evidence of their presence in some of these processes has been observed, by identifying the associated charm jets and showed that this is possible for mass difference Δm above about 10 GeV. A determination of the stop and neutralino masses from the jet/photon plus $\not\!\!E_{\rm T}$ channels seems very challenging. In the future, a more detailed study with a realistic detector simulation should be performed to confirm our results.

Acknowledgments

We would like to thank S. Kraml, A. Raklev, M. Schmitt, T. Sjöstrand and J. Wacker for useful discussions and comments. Work at ANL is supported in part by the US DOE, Division of HEP, Contract DE-AC-02-06CH11357. Fermilab is operated by Universities Research Association Inc. under contract no. DE-AC-02-76CH02000 with the DOE. The authors are thankful to the Aspen Center for Physics, where part of this work has been performed. M. C. and C. W. are grateful to the KITP, Santa Barbara, and the KITPC, Beijing, for hospitality during stages of this work.

References

[1] A.G. Cohen, D. B. Kaplan and A. E. Nelson, Ann. Rev. Nucl. Part. Sci. **43** (1993) 27;
M. Quirós, Helv. Phys. Acta **67**, 451 (1994);
V. A. Rubakov and M.E. Shaposhnikov, Phys. Usp. **39** (1996) 461;
M. Carena and C. E. M. Wagner, hep-ph/9704347;
A. Riotto, M. Trodden, Ann. Rev. Nucl. Part. Sci. **49** (1999) 35;
M. Quirós and M. Seco, Nucl. Phys. B **Proc. Suppl. 81** (2000) 63, hep-ph/9703274.

[2] M. Carena, M. Quirós and C. E. M. Wagner, Phys. Lett. B **380**, 81 (1996);
M. Laine, Nucl. Phys. B **481**, 43 (1996);
M. Losada, Phys. Rev. D **56**, 2893 (1997);
G. Farrar and M. Losada, Phys. Lett. B **406**, 60 (1997);
B. de Carlos and J. R. Espinosa, Nucl. Phys. B **503**, 24 (1997);
D. Bodeker, P. John, M. Laine and M. G. Schmidt, Nucl. Phys. B **497**, 387 (1997);
M. Carena, M. Quirós and C. E. M. Wagner, Nucl. Phys. B **524**, 3 (1998);
M. Laine, K. Rummukainen, Nucl. Phys. B **535**, 423 (1998);
M. Losada, Nucl. Phys. B **537**, 3 (1999) and Nucl. Phys. B **569**, 125 (2000);
M. Laine and M. Losada, Nucl. Phys. B **582**, 277 (2000);
M. Laine and K. Rummukainen, Nucl. Phys. B **597**, 23 (2001).

[3] R. Barate *et al.* [LEP2 Higgs Working Group, ALEPH, DELPHI, L3 and OPAL Collaborations], Phys. Lett. B **565**, 61 (2003);

LEP2 Higgs Working Group, ALEPH, DELPHI, L3 and OPAL experiments, note LHWG-Note-2004-01. [http://lephiggs.web.cern.ch/LEPHIGGS/papers/].

[4] T. Ibrahim and P. Nath, Phys. Rev. D **58**, 111301 (1998) [Erratum-ibid. D **60**, 099902 (1999)];
S. Abel, S. Khalil and O. Lebedev, Nucl. Phys. B **606**, 151 (2001);
D. Chang, W. F. Chang and W. Y. Keung, Phys. Rev. D **66**, 116008 (2002);
A. Pilaftsis, Nucl. Phys. B **644**, 263 (2002).

[5] C. Balázs, M. Carena and C. E. M. Wagner, Phys. Rev. D **70**, 015007 (2004);
C. Balázs, M. Carena, A. Menon, D. E. Morrissey and C. E. M. Wagner, Phys. Rev. D **71**, 075002 (2005).

[6] V. Cirigliano, S. Profumo and M. J. Ramsey-Musolf, JHEP **0607**, 002 (2006).

[7] A. Djouadi, Phys. Lett. B **435**, 101 (1998);
A. Menon and D. E. Morrissey, in preparation.

[8] K. i. Hikasa and M. Kobayashi, Phys. Rev. D **36**, 724 (1987).

[9] V. M. Abazov *et al.* [DØ Collaboration], Phys. Lett. B **665**, 1 (2008).

[10] N. Bhattacharyya, A. Datta and M. Maity, arXiv:0807.0994 [hep-ph].

[11] [CDF and D0 Collaborations], Report to the Particle Physics Project Prioritization Panel: *The Case for Run II* (2005), http://www-cdf.fnal.gov/physics/projections/stop_limit_Run2_CDFD0_1.eps.

[12] S. Kraml and A. R. Raklev, Phys. Rev. D **73**, 075002 (2006);
S. Kraml and A. R. Raklev, AIP Conf. Proc. **903**, 225 (2007) [hep-ph/0609293].

[13] S. P. Martin, arXiv:0807.2820 [hep-ph].

[14] N. Arkani-Hamed, S. Dimopoulos and G. R. Dvali, Phys. Lett. B **429**, 263 (1998);
G. F. Giudice, R. Rattazzi and J. D. Wells, Nucl. Phys. B **544**, 3 (1999).

[15] J. Alwall, M. P. Le, M. Lisanti and J. G. Wacker, arXiv:0803.0019 [hep-ph].

[16] See, for example, L. E. Ibáñez, C. López and C. Muñoz, Nucl. Phys. B **256**, 218 (1985).

[17] R. Dermisek and H. D. Kim, Phys. Rev. Lett. **96**, 211803 (2006);
R. Kitano and Y. Nomura, Phys. Rev. D **73**, 095004 (2006);
R. Essig and J. F. Fortin, JHEP **0804**, 073 (2008).

[18] A. G. Cohen, D. B. Kaplan and A. E. Nelson, Phys. Lett. B **388**, 588 (1996).

[19] N. Arkani-Hamed, S. Dimopoulos, G. F. Giudice and A. Romanino, Nucl. Phys. B **709** (2005) 3.

[20] M. Carena, G. Nardini, M. Quiros and C. E. M. Wagner, arXiv:0806.4297 [hep-ph].

[21] G. Hiller and Y. Nir, JHEP **0803**, 046 (2008).

[22] E. Boos *et al.* [CompHEP Collaboration], Nucl. Instrum. Meth. A **534**, 250 (2004).

[23] T. Sjöstrand, S. Mrenna and P. Skands, JHEP **0605** (2006) 026.

[24] A. S. Belyaev *et al.*, in *Proceedings, Advanced Computing and Analysis Techniques in Physics Research (ACAT 2000)*, eds. P. C. Bhat and M. Kasemann, Amer. Inst. Phys., Melville, N.Y., (2001) [hep-ph/0101232].

[25] T. Sjöstrand, `http://www.thep.lu.se/~torbjorn/pythia/main73.f`;
see also M. Fairbairn, A. C. Kraan, D. A. Milstead, T. Sjöstrand, P. Skands and T. Sloan, Phys. Rept. **438**, 1 (2007).

[26] J. Conway *et al.*, PGS 4, `http://www.physics.ucdavis.edu/~conway/research/software/pgs/pgs4-general.htm`.

[27] G. L. Bayatian *et al.* [CMS Collaboration], *"CMS technical design report, volume II: Physics performance,"* J. Phys. G **34**, 995 (2007), p. 203 ff.;
J. Weng, G. Quast, C. Saout, A. De Roeck, M. Spiropulu, CMS Note 2006/129.

[28] L. Vacavant and I. Hinchliffe, J. Phys. G **27**, 1839 (2001);
L. Vacavant and I. Hinchliffe, ATLAS Note ATL-PHYS-2000-016 [hep-ex/0005033].

[29] W. Beenakker, R. Höpker, M. Spira and P. M. Zerwas, Nucl. Phys. B **492**, 51 (1997).

[30] S. Dittmaier, P. Uwer and S. Weinzierl, Phys. Rev. Lett. **98**, 262002 (2007).

[31] M. Goncharov, talk given at *Pheno 2008 Symposium*, Madison, Wisconsin, USA (28–30 April 2008); see also `http://www-cdf.fnal.gov/physics/exotic/exotic.html`.

[32] DØ Note 5729-Conf [`http://www-d0.fnal.gov/Run2Physics/WWW/results/prelim/NP/N63`].

[33] M. Carena, A. Finch, A. Freitas, C. Milsténe, H. Nowak and A. Sopczak, Phys. Rev. D **72**, 115008 (2005);
A. Freitas, C. Milsténe, M. Schmitt and A. Sopczak, arXiv:0712.4010 [hep-ph].

[34] C. G. Lester and D. J. Summers, Phys. Lett. B **463**, 99 (1999);
A. Barr, C. Lester and P. Stephens, J. Phys. G **29**, 2343 (2003);
W. S. Cho, K. Choi, Y. G. Kim and C. B. Park, Phys. Rev. Lett. **100**, 171801 (2008);
A. J. Barr, B. Gripaios and C. G. Lester, JHEP **0802**, 014 (2008).